



Acoustics'08  
Paris  
June 29-July 4, 2008

[www.acoustics08-paris.org](http://www.acoustics08-paris.org)

*euonoise*

## Direct and modal frequency response analysis of sound fields in small rooms by finite element method

Reiji Tomiku, Toru Otsuru, Noriko Okamoto and Yuka Kurogi

Faculty of Engineering, Oita University, Dannoharu 700, 870-1192 Oita, Japan  
tomiku-reiji@cc.oita-u.ac.jp

In this paper, sound pressures are computed by two techniques using finite element method. One is a technique by solving the system of linear equations directly (direct analysis) and the other is a technique by modal superposition (modal analysis). To confirm the accuracy of the direct analysis, sound pressures obtained by the technique are compared with those obtained by the modal analysis in a room with the volume of  $10 \text{ m}^3$ . Then, as the modal analysis, two methods are employed: one is simplified method based on real eigenvalue problem assuming that the damping matrix,  $[C]$ , has orthogonality; and another is the method based on complex eigenvalue problem. Those obtained by the direct analysis are in good agreement with those obtained by the two kinds of modal analyses regardless of absorption conditions, even if the analysis is carried out at the frequency close to an eigen frequency. Next, diffuseness of sound field below 315 Hz in a room, which is used in the measurement of ISO140-3, is investigated by the direct analysis from the viewpoint of mean sound pressure level measurements.

## 1 Introduction

In recent years, various numerical methods based on the wave acoustics have been proposed to accurately predict a sound field inside buildings [1]. Among these methods, finite element method (FEM) is advantageous in its broad range of adaptability. The method can successfully be applied to such sound fields like one with temperature distribution [2], and so on. The authors presented finite elemental procedure in the former paper [3], which enables us to estimate resulting accuracy of sound field analyses by FEM. The authors have also proved that sound pressure level distributions in an irregularly shaped reverberation room obtained by the authors' FE-analysis were in good agreement with those of measurements on various conditions caused by absorbent materials [4].

Using FEM, sound pressures in steady-state can usually be evaluated by two techniques: one is a technique by solving the system of linear equations directly (direct frequency response analysis, for short, direct analysis); the other is a technique by modal superposition (modal frequency response analysis, for short, modal analysis). Generally, if absorption is small, the direct analysis has mathematical uncertainty at the points close to eigen frequencies of the cavity, although the analysis requires less computational costs.

In this paper, we focus on the relationships between the accuracy of the direct analysis and boundary absorption condition of analytical model. To confirm the accuracy of the direct analysis, sound pressures obtained by the direct analysis are compared with those obtained by the modal analysis. Then, as the modal analysis, two methods are employed: one is the simplified method based on real eigenvalue problem assuming that the damping matrix,  $[C]$ , has orthogonality (MK-type); and another is the method based on complex eigenvalue problem (MCK-type). First, in case of sound fields with absorbent material, absorption coefficients of which are 0.2 or more, sound pressure level distributions obtained by the direct analysis are compared with those obtained by the modal analyses in a small cavity with the volume of  $10 \text{ m}^3$ . Next, to clarify accuracy of the direct analysis when absorption is small, the sound pressure level distributions and frequency responses obtained by the direct analysis are compared with those obtained by the modal analyses in case that all boundaries of analytical model equal 0.01. Finally, as an application to the actual problem, a measurement of a mean sound pressure level in a room is investigated by the direct analysis.

## 2 Finite element sound field analysis of cavities

### 2.1 Basic formulation

Following the standard finite element procedure applied to a three-dimensional wave equation assuming the time constant to be  $e^{i\omega t}$ , discretized equation of motion in frequency domain can be written as below [3]:

$$[K]\{p\} + i\omega[C]\{p\} - \omega^2[M]\{p\} = i\omega\rho v_0\{W\}. \quad (1)$$

In that equation,  $[K]$ ,  $[C]$  and  $[M]$  respectively represent the acoustic stiffness, dissipation and mass matrices;  $\{p\}$  is the sound pressure vector; also  $i$ ,  $\omega$ ,  $\rho$ ,  $v_0$  and  $\{W\}$  respectively represent the imaginary unit, angular frequency, air density, particle velocity and distribution vector. The acoustic element matrices,  $[K]_e$  and  $[M]_e$ , that construct global matrices in the Eq.(1) are given by the equations in the literature [3]. As for the damping matrix,  $[C]_e$ , it can be defined as below:

$$[C]_e = \frac{1}{c} \int \frac{1}{z_n} \{N\}\{N\}^T dS. \quad (2)$$

Therein,  $c$  and  $z_n$  are the sound velocity and normal surface impedance.

### 2.2 Direct frequency response analysis

The Eq.(1) can be rewritten as

$$[A]\{p\} = \{f\}. \quad (3)$$

The coefficient matrix  $[A]$  becomes a complex sparse symmetric matrix, i.e. a non-Hermitian matrix. The  $\{p\}$  can be directly obtained by applying a direct solver or an iterative solver onto the Eq.(3). The solver employed here is COCG method [5], which is the effective iterative solver for the authors' FEM [6].

### 2.3 Modal frequency response analysis

The modal superposition technique by use of FEM becomes simpler when the dissipation is small enough to ignore modal couplings. In this case, simple eigenmodes and eigenvalues derived by solving a MK-type eigen equation can be utilized to the modal superposition technique. So, the following equation was tentatively solved to obtain eigenvalues,  $\omega_n$  and eigen-vectors,  $\{\phi_n\}$  :

$$([K] - \omega_n^2 [M])\{\phi_n\} = 0. \quad (4)$$

With the  $\omega_n^2$  and  $\{\phi_n\}$ ,  $\{p(\omega)\}$  in the steady-state condition can be obtained by modal superposition technique as follows (Modal\_MK):

$$\{p(\omega)\} = \sum_{n=1}^N \alpha_n \{\phi_n\}, \quad (5)$$

where,

$$\alpha_n = \frac{\{\phi_n\}^T \{F\}}{(\omega_n^2 - \omega^2 + i2h_n \omega_n \omega) M_n},$$

$$h_n = \frac{\{\phi_n\}^T [C(\omega_n)] \{\phi_n\}}{2\omega_n M_n}, \quad M_n = \{\phi_n\}^T [M] \{\phi_n\}. \quad (6)$$

The damping matrix,  $[C(\omega)]$  can be decided by putting the impedance value at the frequency  $\omega_n$  into the Eq.(6).

On the other hand, if the dissipation is not small enough, the following MCK-type eigen equation can be utilized:

$$(\omega_n^2 [M] + \omega_n [C] + [K])\{\phi_n\} = 0. \quad (7)$$

The Eq.(7) can be rearranged as follows,

$$(\omega_n [D] + [E])\{\psi_n\} = 0, \quad (8)$$

where,

$$[D] = \begin{bmatrix} C & M \\ M & 0 \end{bmatrix}, \quad [E] = \begin{bmatrix} K & 0 \\ 0 & -M \end{bmatrix}, \quad \{\psi_n\} = \begin{Bmatrix} \phi_n \\ i\omega_n \phi_n \end{Bmatrix}. \quad (9)$$

### 3 Comparison between direct and modal frequency response analyses

#### 3.1 Problem and FE settings

The sound field of a cavity with the volume of  $10 \text{ m}^3$  (Fig. 1) is analyzed by direct analysis and by two modal analyses, i.e. Modal\_MK and Modal\_MCK. The sound source is assumed to radiate a volume velocity of  $i\omega v_0 = 1 \text{ m}^3/\text{s}^2$  at the corner point shown in the Fig. 1. Two kinds of boundary conditions are assumed as follow:

- cond. 1: the absorbent material exists on the floor shown in Fig. 1 and other boundaries are assumed to be typical concrete walls.
- cond. 2: all the boundaries are assumed to be typical concrete wall.

In the paper, the surface impedance,  $z_n$ , corresponding to

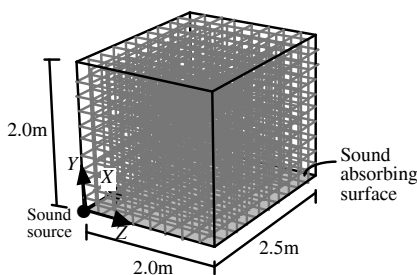


Fig. 1. Schematic drawing of oblong room with a finite element mesh division

$\alpha$	$(z_n[\text{Re}], z_n[\text{Im}])$
0.2	(0.65, -3.20)
0.4	(0.60, -1.86)
0.6	(0.60, -1.19)
0.8	(0.62, -0.69)

Table 1. Normal impedance  $z_n$  of the floor.

absorption coefficient ( $\alpha$ ) equals to 0.01 was given as those of concrete walls assuming that the imaginary part of  $z_n$  is zero. In cond. 1, four absorbent settings are assumed for the absorbent material put on the floor in the room (Table 1).

The finite element employed through this paper is the hexahedron 27-node isoparametric acoustic element [3] using the spline function for the interpolation function. With the element, an array of element is set to  $(X, Y, Z) = (10, 10, 8)$  which satisfies "wave-length" / "nodal-distance"  $> 4.4$  at all frequencies in the following analyses. The *DOF* becomes 7,497.

#### 3.2 Results and discussions

First of all, in case of cond. 1, comparisons among sound pressure levels of all nodes,  $\{L\}$ , obtained by direct analysis, Modal\_MK and Modal\_MCK, are carried out. The sound pressures within the 1/3 octave band centered at frequency 250 Hz were computed at 1 Hz intervals, and square sound pressures of those were integrated.

Figure 2 shows the mean residuals,  $|\bar{D}|$ , between  $\{L\}$  obtained by Modal\_MK and  $\{L\}$  obtained by Modal\_MCK; those between  $\{L\}$  obtained by direct analysis and  $\{L\}$  obtained by Modal\_MCK; those between  $\{L\}$  obtained by direct analysis and  $\{L\}$  obtained by Modal\_MK. The  $|\bar{D}|$  between Modal\_MK and direct-analysis/Modal\_MCK at a higher absorption is larger. In contrast, the  $|\bar{D}|$  between direct analysis and Modal\_MCK are less than 1.0 dB irrespective of boundary conditions.

Comparisons between sound pressure level distributions on the *XZ*-plane ( $Y = 1.0 \text{ m}$ ) obtained by direct analysis and those obtained by Modal\_MCK are shown in Fig. 3 when the  $\alpha$ s of absorbent material equal 0.2 and 0.8. As a reference, those obtained by Modal\_MK are illustrated in the figure. It is confirmed that the sound pressure levels obtained by direct analysis correspond to those obtained by Modal\_MCK regardless of boundary conditions.

Next,  $\{L\}$  obtained by direct analysis are compared with those obtained by modal analysis in the case of cond. 2, i.e. the sound field without absorbent material. The sound pressures within the 1/3 octave band centered at frequency 100-315 Hz were computed at 1 Hz intervals, and square sound pressures of those were integrated.

Figure 4 shows comparisons between sound pressure level

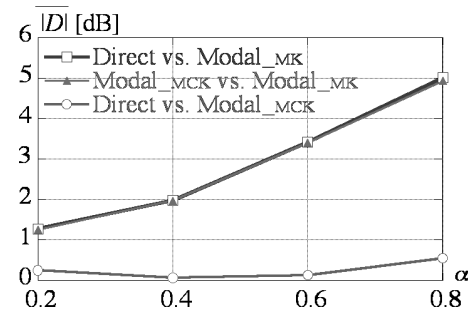


Fig. 2. Mean residuals of sound pressure levels among direct analysis (Direct) and modal analyses: Modal\_MK and Modal\_MCK (cond.1)

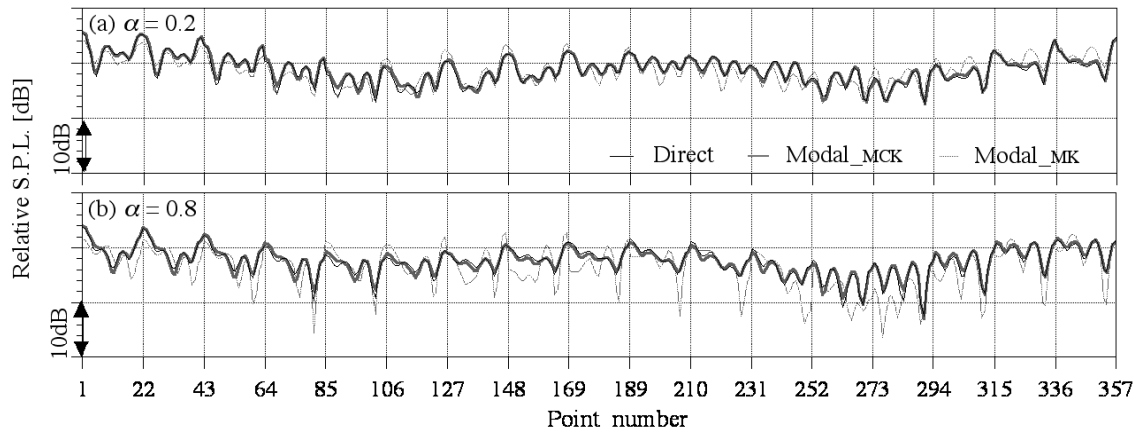


Fig. 3. Comparisons of sound pressure levels among direct analysis (Direct) and two kinds of modal analyses, i.e. Modal\_MK and Modal\_MCK (cond.1); (a)  $\alpha$  of absorbent material equals 0.2, (b)  $\alpha$  of absorbent material equals 0.8

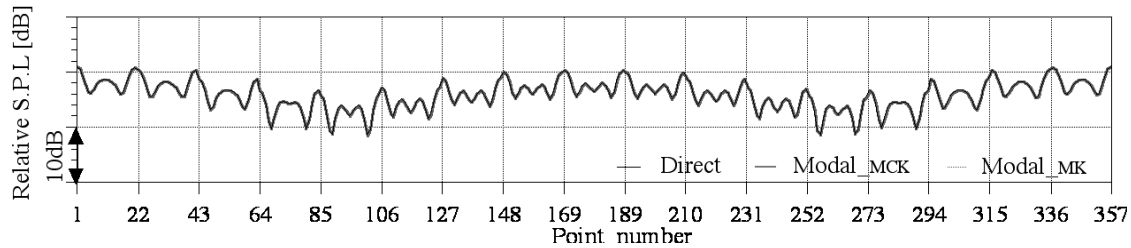


Fig. 4. Comparison of sound pressure levels among direct analysis (Direct) and two kinds of modal analyses, i.e. Modal\_MK and Modal\_MCK (cond.2)

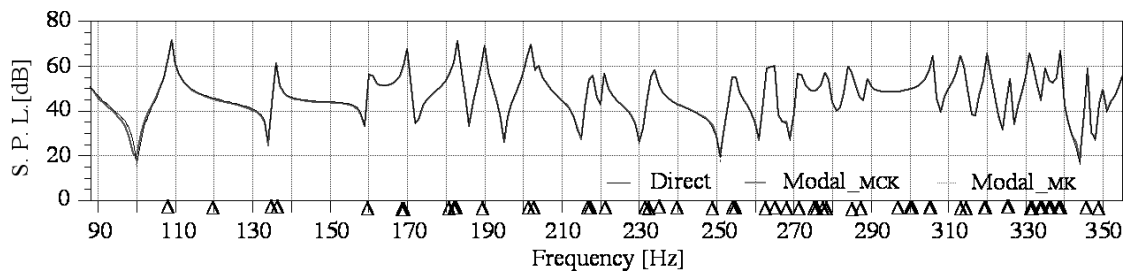


Fig. 5. Comparison of frequency responses among direct analysis (Direct) and two kinds of modal analyses, i.e. Modal\_MK and Modal\_MCK (cond.2)

distributions on the  $XZ$ -plane ( $Y = 1.0$  m) obtained by direct analysis and those obtained by two kinds of modal analyses at 250 Hz. The sound pressure levels obtained by direct analysis are in good agreement with those obtained by both modal analyses. The  $|\bar{D}|$  between  $\{L\}$  obtained by direct analysis and those obtained by both modal analyses is less than 0.1 dB.

Here, frequency responses obtained by direct analysis are compared with those obtained by two kinds of modal analyses in the case of cond. 2. Figure 5 shows frequency responses ranging from 88 Hz to 355 Hz on a point which is (0.5, 1.0, 0.5) obtained by direct analysis and two kinds of modal analyses. Triangular marks ( $\Delta$ ) illustrated in the figure denote eigen frequencies. Results obtained by direct analysis are in good agreement with those obtained by both modal analyses, even if the analysis is carried out at the frequency close to a eigen frequency.

For reference, memory required for Modal\_MCK was 4.6 GB, and that of Modal\_MK was 965 MB whereas that of direct analysis was 7.9 MB. It is concluded that the direct analysis can be regarded as a reasonable one for the computation to obtain a sound pressure distribution in a cavity.

## 4 Investigation on measurement of a mean sound pressure levels in a room

### 4.1 Problem and FE settings

A mean sound pressure level is utilized for several ISO standards and the Japanese Industrial Standards for acoustics. There remain issues caused by differences of sound fields or diffuseness in rooms used for the measurements [7]. On the other hand, the authors presented that data obtained by the finite element analysis were applied to calculate descriptors of diffuseness of sound fields in regularly and irregularly shaped reverberation rooms and showed effectiveness of the method for quantitative evaluations of the sound fields [8]. In this chapter, difference among mean sound pressure levels caused by combinations of sampling points is investigated by combining the analysis and Monte Carlo method in a room with absorptions on boundaries.

An experimental room (ER), volume of which is about 50  $\text{m}^3$ , is analyzed by the direct frequency response analysis in

this chapter, and figure 6 shows a sound source and absorptions locations; Type 0: no absorption boundary (all surfaces are concrete wall), Type 1: an absorption boundary is located on a wall, Type 2: four absorption boundaries are located on two walls, Type 3: eight absorption boundaries are located on three walls and a ceiling. Area of the absorption boundary in Type 1 ~ Type 3 is same and absorption coefficients of the boundaries are supposed for the room's reverberation time ( $T_{60}$ ) to become 1.2 s or 1.9 s calculated by the Sabine's formula. The surface impedance,  $z_n$ , corresponding to absorption coefficient ( $\alpha$ ) equals to 0.01 was given as those of concrete walls assuming that the imaginary part of  $z_n$  is zero.

An array of the element is set to  $(X, Y, Z) = (10, 12, 10)$  which satisfies "wave-length" / "nodal-distance"  $> 4.4$  at all frequencies in the following analyses. The *DOF* becomes 11025 and the frequency range is decided referring to ISO 140-3 Annex C.

### 4.2 Frequency characteristics of mean sound pressure levels

In ISO 140-3, positions and the number of sampling points for averaged sound pressure levels should be decided by followings: (a) distanced from boundaries of a room and from diffuser more than 0.7 m; (b) distanced from sound sources more than 1.0 m; (c) required more than five points which are distributed spatially uniformly; (d) distanced from each other more than 0.7 m. Thus, using sound pressure levels obtained by the authors' FE-analysis, averaged sound pressure levels are calculated by seven steps below based on the Monte Carlo method:

1. Decide the number of sampling points ( $N_s$ ).
2. Decide the number of combinations of sampling points ( $N_c$ ).
3. Divide the space that satisfies both (a) and (b) into  $N_s$  subspaces.
4. Statistically sample one of the points, sound pressure levels of which are obtained by the FE-analysis, in a subspace.
5. Repeat step 4. for all subspaces (total  $N_s$  points are sampled).

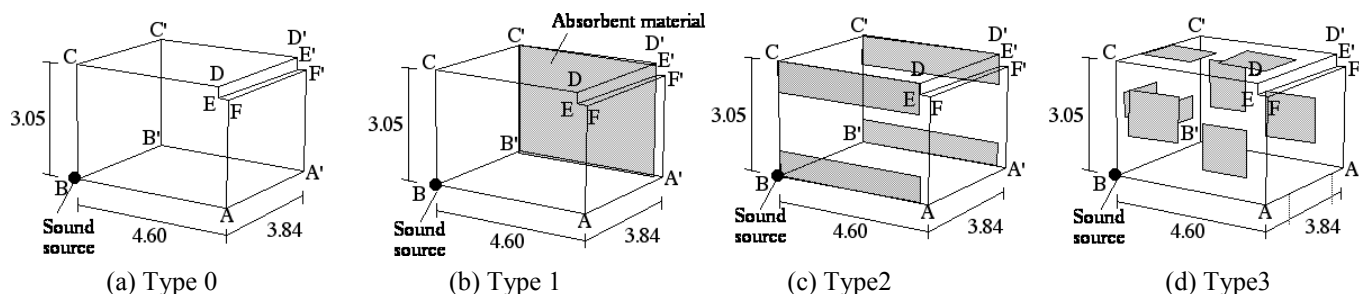


Fig. 6. A sound source and absorptions locations: (a) Type 0; (b) Type 1; (c) Type 2; (d) Type 3 (Unit [m])

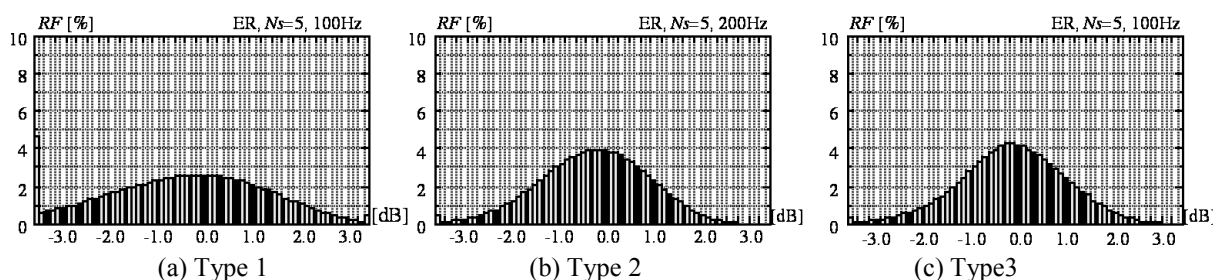


Fig. 7. RF distributions of  $D_n$  at 100 Hz in case that  $N_s = 5$  and  $T_{60} = 1.9$  s.: (a) Type 1; (b) Type 2; (c) Type 3

6. Calculate averaged sound pressure levels by a following equation, if all the  $N_s$  points are distanced from each other more than 0.7 m;

$$L_n = 10 \log \left[ \frac{1}{N} \sum_{k=1}^{N_s} 10^{L_{p,k}(f)/10} \right], \quad (10)$$

where  $L_{p,k}(f)$  is  $L_p(f)$  of  $k$  ( $k = 1, 2, \dots, N_s$ ) and  $n$  is count of calculation of Eq. (10) ( $n = 1, 2, \dots, N_c$ ).

7. Return to step 4 until the  $n$  reaches  $N_c$ .

A difference between  $L_n$  and  $L_{all}$ , which is a mean sound pressure level of all FEM-nodes in the space, which satisfies the both (a) and (b), is calculated by the follow;

$$D_n = L_n - L_{all}. \quad (11)$$

Figure 7 shows relative frequency (*RF* %) distributions of  $D_n$  at 100 Hz in case that  $N_s = 5$  and  $T_{60} = 1.9$  s. The frequencies are counted every 0.1 dB width from -3.0 dB to +3.0 dB and cumulative frequencies are counted under -3.0 dB and over +3.0 dB. It is shown that the *RF* of  $D_n$  around 0.0 dB in Type 2 and Type 3 are higher, *i.e.* the number of  $L_n$  near the  $L_{all}$  is greater, than those in Type 1. To evaluate the difference among mean sound pressure levels caused by combinations of sampling points, cumulative relative frequency of  $D_n$  in case that  $|D_n| < 0.5$  dB (*CRF0.5* %) is calculated. Based on former paper [9], the number of monte carlo trials ( $N_c$ ) is assumed to be  $10^6$ .

### 4.3 Results and discussions

In ISO 140-3, the reverberation time of an experimental room should be within the range of one-two seconds. Thus, relationships between differences among mean sound pressure levels caused by combinations of sampling points and the reverberation times of the room are investigated.

Figure 8 shows relationships between the *CRF0.5* and absorption conditions at 100, 125, 160 and 200 Hz in case that  $N_s = 5$ . It is confirmed that *CRF0.5* in the room with absorptions (Type 1 – 3) are larger than those in the room without absorptions (Type 0) at 100 Hz regardless of the absorption conditions and  $T_{60}$ . On the other hand, *CRF0.5* in the room with absorptions are smaller than those in the room without absorptions at 160 and 200 Hz regardless of

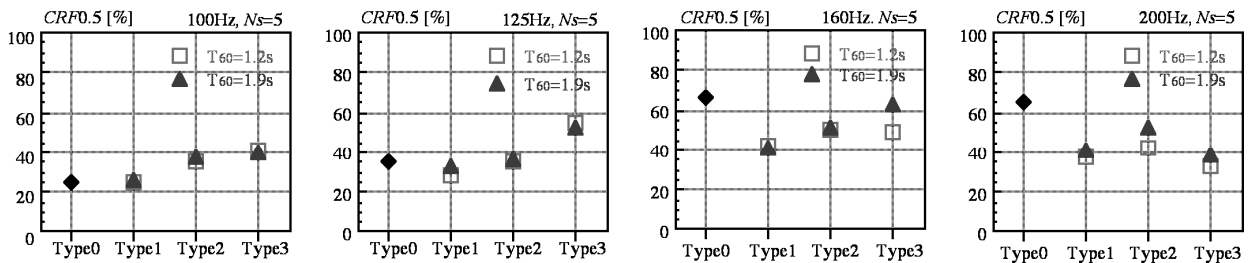


Fig. 8. Comparison between  $CRF0.5$  and absorption conditions at 100, 125, 160 and 200 Hz in case that  $N_s = 5$

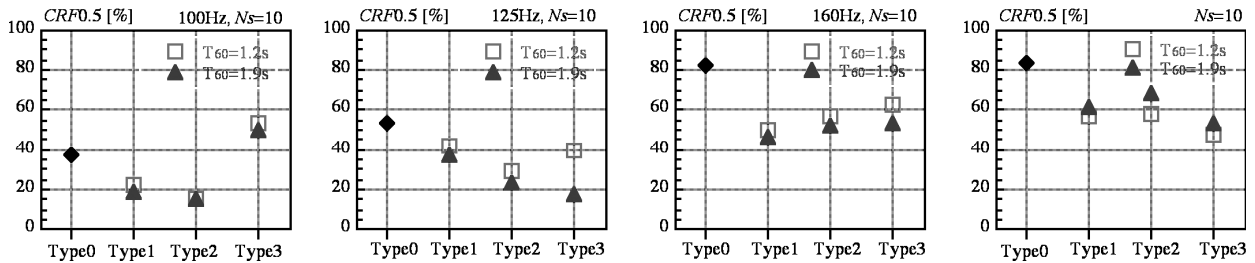


Fig. 9. Comparison between  $CRF0.5$  and absorption conditions at 100, 125, 160 and 200 Hz in case that  $N_s = 10$

the absorption conditions and  $T_{60}$ . At 125 Hz,  $CRF0.5$  in Type 3 is larger than those in Type 0 though those in Type 1 and Type 2 are smaller than those in Type 0 regardless of  $T_{60}$ .

Relationships between  $CRF0.5$  and absorption conditions at 100, 125, 160 and 200 Hz in cases that  $N_s = 10$  are shown in Fig. 9. It is confirmed that  $CRF0.5$  in case that  $N_s = 10$  are larger than those in case that  $N_s = 5$  regardless of the frequency and the boundary condition. At 100 Hz,  $CRF0.5$  in Type 3 is larger than those in Type 0 though those in Type 1 and Type 2 are smaller than those in Type 0 regardless  $T_{60}$ .  $CRF0.5$  in the room with absorptions are smaller than those in the room without absorptions at 125, 160 and 200 Hz regardless of the absorption conditions and  $T_{60}$ . It is noted that adjustments of reverberation time of the experimental room above 125 Hz increase differences among measurement results of mean sound pressure levels.

## 5 Summary

Sound pressures obtained by finite element method with the technique to solve the system of linear equations directly (direct analysis) are compared with those using modal superposition technique (modal analysis) under five kinds of absorption conditions. Results obtained by direct analysis are in good agreement with those obtained by modal analysis regardless of absorption conditions. It is concluded that the direct analysis can be regarded as a reasonable one for the computation to obtain a sound pressure distribution in a room.

## Acknowledgments

This work was supported by Grant-in-Aid for Scientific Research (A) 19206062. The computation was mainly carried out using the computer facilities at the Computing and Communications Center of Kyushu University.

## References

- [1] <http://gacoust.hwe.oita-u.ac.jp/AIJ-BPCA/>.
- [2] T. Otsuru, R. Tomiku, Y. Takahashi, M. Toyomasu, "Large scale sound field analysis by finite element method applied onto rooms with temperature distribution", *Proc. of 9th International Congress on Sound and Vibration, Orlando*, CD-ROM (2002. 7)
- [3] T. Otsuru, R. Tomiku, "Basic characteristics and accuracy of acoustic element using spline function in finite element sound field analysis", *J. Acoust. Soc. of Jpn(E)* 21, No.2, 87-95 (2001)
- [4] R. Tomiku, T. Otsuru, "Sound fields analysis in an irregular shaped reverberation room by finite element method", *J. Archit. Plan. Environ. Eng.* 551, 9-15 (2002) (in Japanese)
- [5] H. A. van der Vorst, J. B. M. Melissen, "A Petrov-Galerkin type method for solving  $Ax = b$ , where  $A$  is symmetric complex", *IEEE Trans. on Magn.* 26, 706-708 (1990)
- [6] N. Okamoto, T. Otsuru, R. Tomiku, T. Okuzono, "Performance of iterative methods and acceleration of computation for large scale finite element sound field analysis in rooms", *Proc. of WESPAC*, CD-ROM (2006)
- [7] Ben H. Sharp, "A Perspective on Noise Control Technology and its future implementation", *Proc. Inter-Noise 99*, 1-4, Dec (1999)
- [8] R. Tomiku, T. Otsuru, Y. Takahashi, "Finite element sound field analysis of diffuseness in reverberation rooms", *JAABE*, 1(2), 33-39 (2002)
- [9] R. Tomiku, T. Otsuru, "Finite Element Sound Field Analysis for a measurement of an averaged sound pressure levels in rooms", *inter-noise2005*, CD-ROM (2005)